

# Design and development of a 4DOFs micro-manipulator

Paolo Righettini<sup>1</sup>, Bruno Zappa<sup>1</sup>, Andrea Ginammi<sup>1</sup>, Alessandro Gotti<sup>1</sup>, Davide Donadini<sup>1</sup>, Roberto Strada<sup>1</sup>

<sup>1</sup>*Dipartimento di Ingegneria, Università degli Studi di Bergamo, Italy*

*E-mail: paolo.righettini@unibg.it, bruno.zappa@unibg.it, andrea.ginammi@unibg.it, alessandro.gotti@unibg.it, davide.donadini@unibg.it, roberto.strada@unibg.it*

*Keywords:* Micro manipulation, micro motors, mechatronics.

**SUMMARY.** This paper describes the research activity of the authors within the National Relevance Project (PRIN2009) “Project Micro Manipulation and Assembly MM&A”, which concerns manipulation and assembly of extremely small components. In particular, the design process and development of a 4–DOFs parallel hybrid manipulator is presented. A mechatronic approach to the kinematic and dynamic synthesis of the micro-manipulator is presented and discussed, focusing also on the integration of the drive systems within the mechanical frame, with particular reference to the choice of the proper motor/transmission units to get the required performances. After the design phase, according to the choices made, a preliminary prototype of the device has been realized; relevant experimental tests will be carried on soon in order to investigate the characteristics and validate the performances of the proposed micro-manipulator.

## 1 INTRODUCTION

The growing trend of miniaturization can be observed in several industrial sectors; while some devices (for example MEMS devices) require no or little assembly other miniaturized products can be composed by several parts that have to be manipulated and assembled. Many of these micro-products are still mounted manually by a skilled human operator raising the production costs [1]. For an automated assembly system, the principal and most demanding functionality is manipulation, placement and assembly of the various parts. Thus the manipulator plays a key role in an automated assembly system for micro components. Conventional commercial manipulator used for micro assembly can be classified into serial, parallel, and hybrid structure. Among serial manipulators used in this field we can mention the Cartesian Sysmelec Autoplace that can reach a repeatability better than 3 microns but it is extremely large in comparison to the element to be manipulated, and several commercial SCARA robots, for instance the *Mitsubishi Melfa RH-6SH5520*, the *Yamaha Yk120X*, the *Bosh Turboscara SR4* and the *Epson E2C251*. On average, they have a large workspace with respect to their size, but repeatability is quite low. As regards fully parallel and hybrid robots for micro-manipulation, they are not so widespread in industrial field, while there are several ongoing research projects covering this area. For example, the *Asyrl Pocket Delta* has a repeatability better than  $2.5\mu m$ . The four axes parallel hybrid *Mitsubishi Melfa RP-IAH* can achieve a repeatability of  $5\mu m$ . Among the scientific projects in this area, we mention the Triglide robot [3], which has a repeatability better than  $1\mu m$ , the parallel hybrid robot Parvus [2, 4] and the Dexter robot [5]. An open problem concerning the miniaturization of these structures is the difficulty to achieve suitable performances such as accuracy and repeatability in positioning. The use of parallel kinematics structure in small scale robots seems to be promising for their characteristics such as high stiffness, compact-structure, and high precision [6, 7]. Moreover, another advantage of these small scale manipulators is that actuators are not a part of the moving mass. The drawback of parallel structures is the high number of joints: this may result in a decreasing precision due to backlash and friction in joints [2].

As regards the drive systems, in recent years, highly dynamic micro-servomotors (e.g. Faulhaber and Maxon Motor), micro-planetary gears (e.g. Faulhaber and Micromotion) and “zero-backlash” Harmonic-Drive have been developed and are commercially available.

This paper describes the research activity carried out by the University of Bergamo within the PRIN2009 “Project Micro Manipulation and Assembly MM&A” in the field of robotized micro manipulation and assembly of extremely small components.

The purpose of the research activity is to contribute to the realization of automatic assembly systems for handling micro parts. In particular, the project aims to develop: innovative micro grippers; innovative positioning and orienting systems with accuracy and repeatability of few microns and overall dimensions of few centimeters; monitoring systems for pieces recognition and devices calibration and supervision [8].

In this contest the research group of the University of Bergamo is in-charge of design and develop a mini manipulator able to accurately and precisely position the micro parts.

This activity involves, in addition to the manipulator mechatronic design, also the development of a specific mini-manipulator that will be integrated in the final demonstrator, a mini work cell where the developed devices will cooperate to automatically execute the required micro-assembly tasks.

A preliminary robot prototype has been realized and experimental tests will soon be conducted in order to verify the performances and the characteristics of the presented manipulator.

## 2 DESIGN REQUIREMENTS AND KINEMATIC ARCHITECTURE

The basic kinematic and dynamic design requirements for the miniaturized assembly robot can be summarized as follow:

- the manipulator have to provide *4 degrees of freedom* and guarantee translational motion along three orthogonal axes ( $x$ ,  $y$  and  $z$ ) for the positioning of micro-parts in Cartesian space and a rotation  $\alpha$  around the  $z$ -axis for their orientation (Shoeflies motion);
- the manipulator workspace must contain a prismatic volume whose projection on the  $xy$ -plane is a  $100 \times 35$  mm rectangle, and its extension along  $z$  direction is  $20$  mm; in figure 2 can be seen the pick up area, where the micro-parts have to be grasped, and the release zone where the object must be inserted into holes of different shapes [8];
- the manipulator theoretical repeatability in the  $xy$ -plane should be less than  $10$   $\mu$ m, while its resolution should be around  $2$   $\mu$ m;
- the rated payload of the robot should be at least  $10$  g, while the maximum payload that the manipulator can lift is ( $100$  g).
- Considering the dynamic performance, the robot should execute the pick-and-place test cycle of figure 2 with a frequency of about  $1$  Hz, for the rated payload, while the prescribed cycle time is about  $10$  s for the maximum payload.

On the basis of the required specifications, and after having analyzed several industrial and research miniaturized-robots, as mentioned in section 1, a parallel hybrid kinematic structure was selected (see Figure 1). In particular, the motion in the  $xy$ -plane is obtained by five bar parallel structure (axes 1 and 2); the motion along the  $z$ -axis is realized by means of a ball screw (axis 3) which is integrated in the base frame of the manipulator, in this way the whole parallel structure is moved in  $z$  direction.

Finally, the end-effector absolute rotation  $\alpha$  is assured by axis 4. A servomotor, located on the link 3, drives the axis through a spur gear pair (see Figure 1).

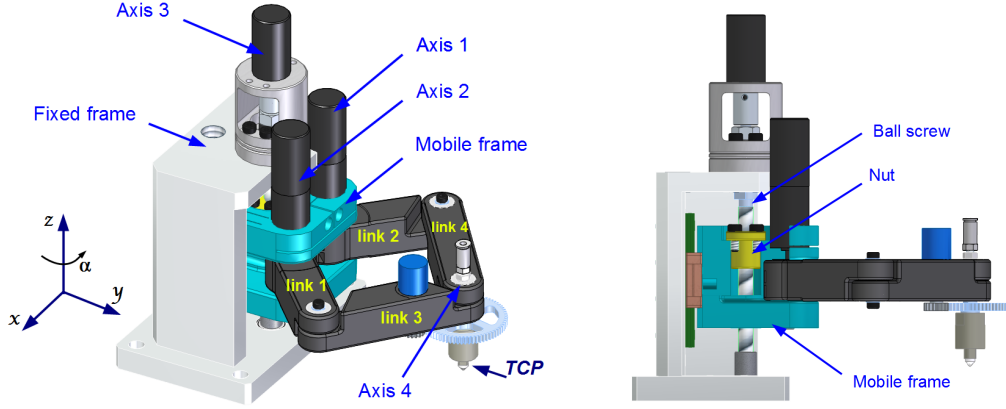


Figure 1: Virtual prototype of the manipulator. Perspective drawing and side view

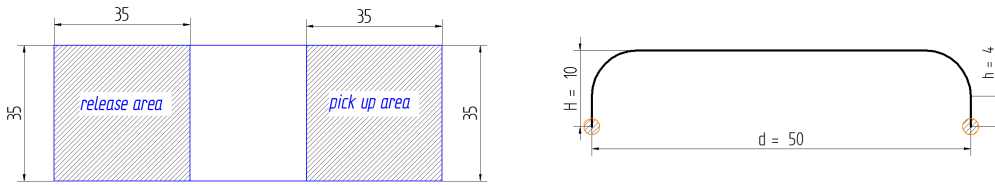


Figure 2: Sketch of the pick up and release working areas and the reference *pick and place* cycle

### 3 KINEMATIC AND DYNAMIC MODEL

In this section, the kinematic and dynamic model of the 4-DOFs manipulator is summarized. We indicate with  $\mathbf{X} = [x_E \ y_E \ z_E \ \alpha]^T$  the pose of the end-effector while  $\mathbf{Q} = [q_1 \ q_2 \ q_3 \ q_4]^T$  is the vector of the joints' rotations; where  $q_1$  and  $q_2$  are the rotation of the actuated joints of the parallel structure,  $q_3$  is the rotation of the ball screw and  $q_4$  is the relative rotation of the end-effector with respect to the moving arm (*link 3* in Figure 1).

#### 3.1 Forward Kinematics

The forward kinematics problem consists in getting the pose (position and orientation) of the end-effector of the manipulator from its actuated articular coordinates (assigned vector  $\mathbf{Q}$ ). For parallel robots the forward kinematics is generally more complex than the inverse problem and can have more than one solution. For this manipulator, thanks to the simplicity of its parallel structure, the admitted solutions can be easily expressed in closed-form. With reference to figure 3(a) the following expressions arise:

$$\begin{cases} x_E = x_A + b \cos \phi_1 \\ y_E = y_A + b \sin \phi_1 \end{cases} \quad \text{with} \quad \begin{cases} \phi_1 = \delta_1 + \psi \\ \psi = \arctan2(y_B - y_A, x_B - x_A) \end{cases} \quad (1)$$

The position of passive joints  $A$  and  $B$  can be expressed as a function of joints' coordinates  $q_i$ :

$$\begin{cases} x_A = a \cos q_1 - \frac{d}{2} \\ y_A = a \sin q_1 \end{cases} \quad \text{and} \quad \begin{cases} x_B = a \cos q_2 + \frac{d}{2} \\ y_B = a \sin q_2 \end{cases} \quad (2)$$

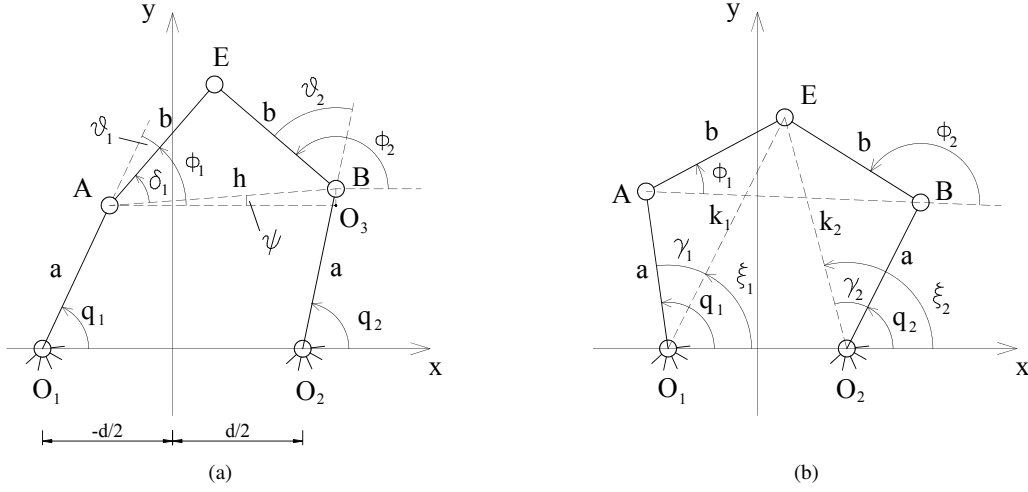


Figure 3: Schematics of the 2-DOF symmetric parallel structure. The actuated joints are  $O_1$  and  $O_2$ , the arms lengths are  $a$  and  $b$ , and the point  $E$  represents the end-effector.

Applying Carnot's theorem to triangle  $AEB$  we get:

$$\delta_1 = \pm \arccos \left( \frac{h}{2b} \right) \quad \text{where} \quad h = \sqrt{(y_B - y_A)^2 + (x_B - x_A)^2} \quad (3)$$

The sign  $\pm$  in equation 3 depends on the chosen assembly mode, in this case two solutions can be obtained for the pose of the end-effector. Moreover, the argument of function  $\arccos$  must be  $-1 \leq \frac{h}{2b} \leq 1$ , thus the links length has to be:  $b \geq \frac{h}{2}$ . Finally, the coordinate  $z_E$  and the absolute rotation  $\alpha$  of the end-effector can be simply written as:

$$z_E = p q_3 \quad \alpha = \phi_2 + q_4 \quad (4)$$

where  $p$  is the pitch of the ball screw.

### 3.2 Inverse Kinematics

The inverse kinematic problem consists in finding the active joints' coordinates (vector  $\mathbf{Q}$ ) for a assigned position and orientation of the end-effector.

Following an approach similar to the one used in the previous section, the kinematic problem can be simply solved. With reference to figure 3(b) it can be written:

$$\begin{cases} q_1 = \xi_1 + \gamma_1 \\ q_2 = \xi_2 - \gamma_2 \end{cases} \quad \text{where} \quad \begin{cases} \xi_1 = \arctan2 \left( y_E, x_E + \frac{d}{2} \right) \\ \xi_2 = \arctan2 \left( y_E, x_E - \frac{d}{2} \right) \end{cases} \quad (5)$$

Applying Carnot's theorem to triangles  $AEO_1$  and  $BEO_2$  the following equations arise:

$$\begin{cases} \gamma_1 = \pm \arccos \left( \frac{a^2 + k_1^2 - b^2}{2ak_1} \right) \\ \gamma_2 = \pm \arccos \left( \frac{a^2 + k_2^2 - b^2}{2ak_2} \right) \end{cases} \quad \text{where} \quad \begin{cases} k_1 = \sqrt{\left( x_E + \frac{d}{2} \right)^2 + y_E^2} \\ k_2 = \sqrt{\left( x_E - \frac{d}{2} \right)^2 + y_E^2} \end{cases} \quad (6)$$

Depending on the sign chosen for  $\gamma_1$  and  $\gamma_2$  (see Eq. 6) four different solutions can be obtained.

As far as the joint coordinates  $q_3$  and  $q_4$  are concerned, they can be written as:

$$q_3 = \frac{z_E}{p} \quad q_4 = \alpha - \phi_2 \quad (7)$$

### 3.3 Velocity and acceleration analysis

The forward kinematics position equations previously stated, can be written in matrix form:

$$\mathbf{X} = \mathcal{F}(\mathbf{Q}) \quad (8)$$

Starting from these equations and differentiating them with respect to time, a set of linear equations are obtained:

$$\dot{\mathbf{X}} = \mathbf{J} \dot{\mathbf{Q}} \quad (9)$$

where  $\dot{\mathbf{X}} = [\dot{x}_E \ \dot{y}_E \ \dot{z}_E \ \dot{\alpha}]^T$  is the generalized velocity of the end-effector,  $\dot{\mathbf{Q}} = [\dot{q}_1 \ \dot{q}_2 \ \dot{q}_3 \ \dot{q}_4]^T$  is a 4-dimensional vector representing the joints' velocities, and  $\mathbf{J}(\mathbf{Q})$  is the  $4 \times 4$  jacobian matrix of the system.

Differentiating Eq. 9 with respect to time, we get the relationship between the generalized acceleration of the end-effector and the joints' accelerations:

$$\ddot{\mathbf{X}} = \mathbf{J} \ddot{\mathbf{Q}} + \frac{d\mathbf{J}}{dt} \dot{\mathbf{Q}} = \mathbf{J} \ddot{\mathbf{Q}} + \dot{\mathbf{J}} \dot{\mathbf{Q}} \quad (10)$$

### 3.4 Dynamics

The rigid body dynamic model of the system has been derived applying the *principle of virtual power*. The friction force acting on the joints and the friction torque in transmissions have been considered, moreover the gravity forces are the only external actions taken into account.

The motion of each rigid body constituting the system can be described by means of the center of mass coordinates  $x_{G_i}$ ,  $y_{G_i}$ ,  $z_{G_i}$ , and the absolute rotation  $\vartheta_i$  around the center of mass itself.

The inertial actions acting on the link  $i$ , whose mass is  $m_i$  and its moment of inertia is  $J_i$ , can be written in matrix form as:

$$\mathbf{F}_{I_i} = -\mathbf{M}_i \ddot{\mathbf{X}}_i \quad (11)$$

where:

$$\mathbf{F}_{I_i} = [F_{x_i} \ F_{y_i} \ F_{z_i} \ C_{I_i}]^T \quad \mathbf{M}_i = \begin{pmatrix} m_i & 0 & 0 & 0 \\ 0 & m_i & 0 & 0 \\ 0 & 0 & m_i & 0 \\ 0 & 0 & 0 & J_i \end{pmatrix} \quad \ddot{\mathbf{X}}_i = [\ddot{x}_{G_i} \ \ddot{y}_{G_i} \ \ddot{z}_{G_i} \ \ddot{\vartheta}_i]^T$$

Considering all the bodies of the system (e.g. the links, the mobile frame, the payload, etc. ), the generalized inertia force, the generalized acceleration and the generalized mass matrix of whole the system can be written as:

$$\begin{aligned} \mathbf{F}_I &= [F_{x_1} \ F_{y_1} \ F_{z_1} \ C_{I_1} \ \dots \ F_{x_n} \ F_{y_n} \ F_{z_n} \ C_{I_n}]^T \\ \ddot{\mathbf{X}} &= [\ddot{x}_{G_1} \ \ddot{y}_{G_1} \ \ddot{z}_{G_1} \ \ddot{\vartheta}_1 \ \dots \ \ddot{x}_{G_n} \ \ddot{y}_{G_n} \ \ddot{z}_{G_n} \ \ddot{\vartheta}_n]^T \\ \mathbf{M} &= \text{diag}(m_1, m_1, m_1, J_1, \dots, m_n, m_n, m_n, J_n) \end{aligned}$$

Applying the *principle of virtual power*, including among the working actions (i.e. the force that produce virtual power) also the inertial ones, the following matrix equation arises:

$$\dot{\mathbf{Q}}^{*T} \mathbf{F}_q + \dot{\mathbf{X}}^{*T} \mathbf{F}_I + \dot{\mathbf{X}}_w^{*T} \mathbf{F}_w = 0 \quad (12)$$

where:  $\mathbf{F}_q = [C_1 \ C_2 \ C_3 \ C_4]^T$  is the vector of the joints' actuating torques,  $\dot{\mathbf{Q}}^*$  contains the joints' virtual velocities,  $\dot{\mathbf{X}}^*$  is the vector of the virtual generalized velocities of the system, while  $\mathbf{F}_w$  and  $\dot{\mathbf{X}}_w^*$  are the generalized "working" actions and their generalized virtual velocity respectively. Vector  $\mathbf{F}_w$  contains the gravity forces and the other working actions acting on the systems (in our case the friction forces).

Expressing the virtual velocities  $\dot{\mathbf{X}}^*$  and  $\dot{\mathbf{X}}_w^*$  as function of  $\dot{\mathbf{Q}}^*$ , leads to:

$$\dot{\mathbf{X}}^* = \frac{\partial \mathbf{X}}{\partial \mathbf{Q}} \dot{\mathbf{Q}}^* = \mathbf{J}_D \dot{\mathbf{Q}}^* \quad \dot{\mathbf{X}}_w^* = \frac{\partial \mathbf{X}_w}{\partial \mathbf{Q}} \dot{\mathbf{Q}}^* = \mathbf{J}_w \dot{\mathbf{Q}}^* \quad (13)$$

where  $\mathbf{J}_D$  is the jacobian matrix which maps the joint rates into the generalized velocities of the bodies, analogously  $\mathbf{J}_w$  relates the joint velocities to the velocities of the "working force".

The generalized actual acceleration of the system is:

$$\ddot{\mathbf{X}} = \mathbf{J}_D \ddot{\mathbf{Q}} + \frac{d\mathbf{J}_D}{dt} \dot{\mathbf{Q}} = \mathbf{J}_D \ddot{\mathbf{Q}} + \dot{\mathbf{J}}_D \dot{\mathbf{Q}} \quad (14)$$

Substituting Eqs. 13 and 14 in Eq. 12 leads to:

$$\mathbf{F}_q = \mathbf{J}_D^T \mathbf{M} \mathbf{J}_D \ddot{\mathbf{Q}} + \mathbf{J}_D^T \mathbf{M} \dot{\mathbf{J}}_D \dot{\mathbf{Q}} - \mathbf{J}_w^T \mathbf{F}_w \quad (15)$$

where  $\mathbf{J}_D^T \mathbf{M} \mathbf{J}_D$  is the (4×4) inertia matrix of the system, vector (4×1)  $\mathbf{J}_D^T \mathbf{M} \dot{\mathbf{J}}_D \dot{\mathbf{Q}}$  contains the velocity-dependent inertia forces (Coriolis and centrifugal) and vector (4×1)  $\mathbf{J}_w^T \mathbf{F}_w$  holds the contribution of the working forces. Hence, equation 15 allows to find the joints' torques needed to properly move the end-effector according to a specific law of motion.

#### 4 KINEMATIC AND DYNAMIC SYNTHESIS

The first part of the research activity was mainly focused on defining the most suitable methods for the kinematic and dynamic synthesis of miniaturized-robot. These methodologies were implemented in a optimization software written in *Matlab*.

By means of the developed software package, an optimization process was carried out in order to determine a "best" solution for the geometric and structural dimensions of the links of the planar structure, and to select the actuators and their mechanical transmissions. This process was subjected to the following constraints: the manipulator has to satisfy the workspace requirements with limited overall dimension, it must exhibit a high degree of dexterity in the working area and fulfill the dynamic requirements (it must accomplish the reference pick-and-place task with the prescribed frequency as specified in section 2). The optimization code allows to monitor several kinematic and dynamic performance indices varying the design parameters. These indices are computed at all points in the reachable workspace and in the prescribed rectangular manipulation area their minimum, maximum and average values are evaluated. More in details, among others, it is possible to calculate some local and global dexterity indices such as the condition number  $\kappa$  of the jacobian matrix  $\mathbf{J}_p$  of the parallel structure and a kinematic manipulability measure. As an example, Figure 4 shows the condition number and the manipulability measure in the *xy* plane for the optimized manipulator depicted in Figure 6 (the colored area corresponds to the reachable workspace with condition number less than 2).

The condition number is defined as the square root ratio between the maximum and the minimum eigenvalues of matrix  $\mathbf{J}_p \mathbf{J}_p^T$  (that corresponds to the ratio between the maximum and the minimum singular values of  $\mathbf{J}_p$ ), while the adopted manipulability measure is the square root of the minimum eigenvalue of  $\mathbf{J}_p \mathbf{J}_p^T$ .

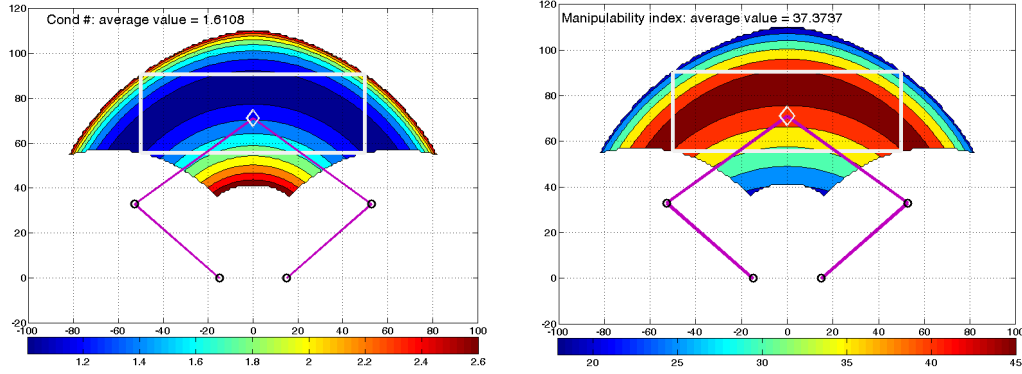


Figure 4: Condition number  $\kappa$  and kinematic manipulability index  $I_M$  for the optimized robot. The solid line rectangle represents the prescribed working area. In this zone the mean value of  $\kappa$  is around 1.7, while the average value of  $I_M$  is greater than 37 mm

Another useful measure taken into consideration in the design phase was the positioning sensitivity in the workspace (i.e. the uncertainty of the robot's pose caused by uncertainty in the position of the joints). Figure 5 shows the sensitivity in X and Y direction defined respectively as the sum of the absolute values of the terms in the first and second row of  $\mathbf{J}_p$ , hence:  $S_x = \sum_{c=1}^2 |J_{1,c}|$  and  $S_y = \sum_{c=1}^2 |J_{2,c}|$ .

For the optimized manipulator the average value of  $S_x$  in the working area is about 58 mm/rad, while of  $S_y$  is less than 62 mm/rad. Thus, assuming a position sensor resolution  $r_M$  of 3000 pulses per revolution, a gearbox with a reduction ratio  $i_R$  of 66/1 (see section 5), we obtain an average end-effector resolution in the Cartesian space of about 2  $\mu$ m:

$$r_W = S_y \frac{2\pi}{i_r r_M}$$

Furthermore, we define the overall sensitivity  $S_{xy}$  as  $S_{xy} = \sqrt{S_x^2 + S_y^2}$ ; its mean value inside the prescribed working area is less than 91 mm/rad. This measure can be useful to estimate the influence of the transmission system inaccuracy (e.g. backlash, hysteresis, etc) on the manipulator pose. For instance, in order to obtain the prescribed repeatability (less than 10  $\mu$ m) the gearbox must have a position accuracy better than 0.063°.

As far as the dynamic requirements are concerned, assigning a reasonable mass distribution to the system, and a suitable motion law that allow to execute the prescribed pick-and-place cycle with the assigned frequency, it is possible to compute the torque exerted on the joints and to preliminary select the drive systems from an assigned database containing the main data of the candidate motors and transmissions. The method adopted for the selection of the actuation systems, an extension of [10], guarantees that the required dynamic performances are satisfied while other characteristics, such as weight, size, peak power, etc., are optimized.

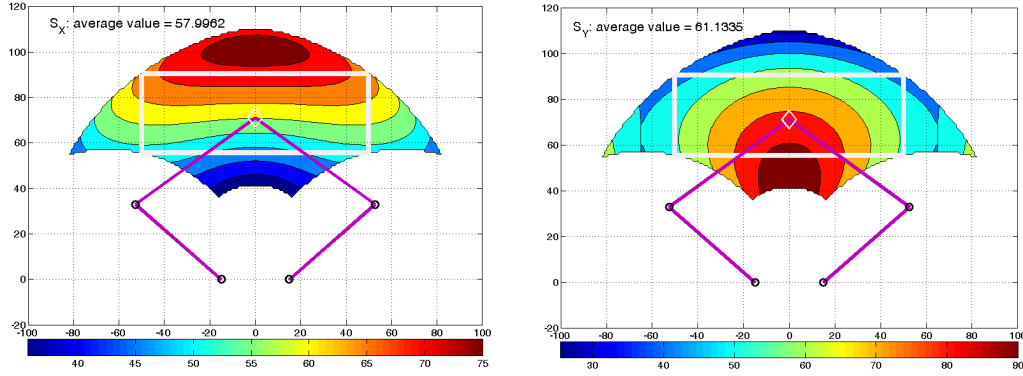


Figure 5: Sensitivity in X and Y direction for the optimized robot. The solid line rectangle represents the prescribed working area

## 5 EXPERIMENTAL SET-UP

In order to test the dynamic performance of the designed manipulator, to verify the adopted control strategies and to tune the measurement system for evaluating its performance (e.g. position accuracy and repeatability according to the UNI-EN-ISO 9283:199 standard), a preliminary prototype of the hybrid manipulator has been realized. Figure 6 depicts the virtual prototype of the manipulator (on the left) and the preliminary realized prototype. The main robot geometrical dimensions of the optimized parallel structure are illustrated in Figure 6 ( $a=65mm$ ,  $b=50mm$ ,  $d=30mm$  and footprint  $100 \times 65mm$ ), while the allowed range of motion of axes 1 and 2 are respectively:  $40^\circ \leq q_1 \leq 189.5^\circ$  and  $-9.5^\circ \leq q_2 \leq 140^\circ$ .

The base frame of the prototype is made of aluminum, while the links and the mobile frame are made of “Vero White Polyjet Resin (FC830)” and fabricated in rapid prototyping.

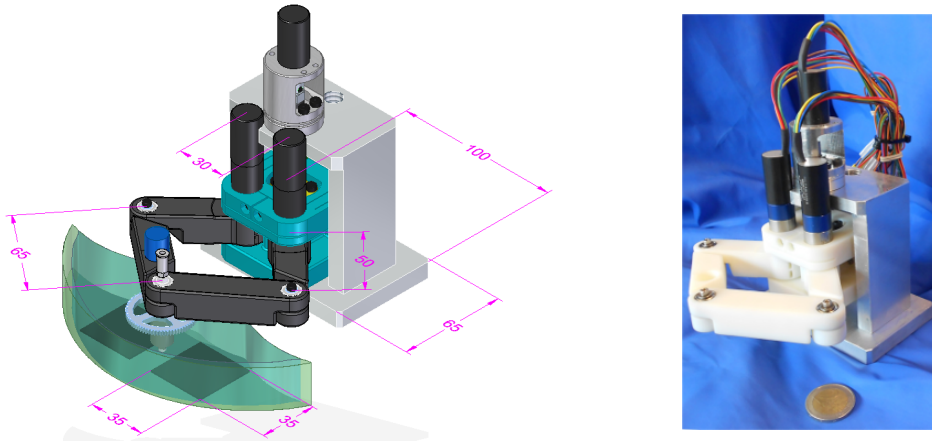


Figure 6: Virtual prototype of the optimized 4-DOF robot. a) Main dimensions, footprint and its working space b) Preliminary physical prototype of the manipulator

The parallel structure is actuated, at the active joints, by two *Faulhaber 1628-T024B* servomotors combined with planetary gearheads with reduction ratio  $66:1$ . The rotation of the end effector is

driven by a *Faulhaber 1226-T012B* brushless servomotor coupled with a planetary reducer (gear ratio  $16:1$ ). Finally, another *Faulhaber 1628-T024B* drives a *NSK* mini ball screw (pitch  $1\text{ mm}$ ) which is integrated in the base frame of the manipulator and moves the whole parallel structure in  $z$  direction. All servomotors are equipped with analog Hall sensors with a resolution of  $3000\text{ pulses/rev}$ . For the control of the manipulator four *Faulhaber MCBL-3002* motion controller with CANopen interface have been selected; the control program has been written in *C++* and has been development on a real-time framework cooperating with the Linux kernel (*Xenomai*)

At the present stage of the research, the manipulator prototype has been realized and the experimental phase will soon begin to test the control algorithms and to verify the performance of the system. At the same time, by means of a finite element analysis, we are designing new manipulator arms made of aluminum alloy in order to get an optimal balance between the lightness of the parallel structure and its stiffness.

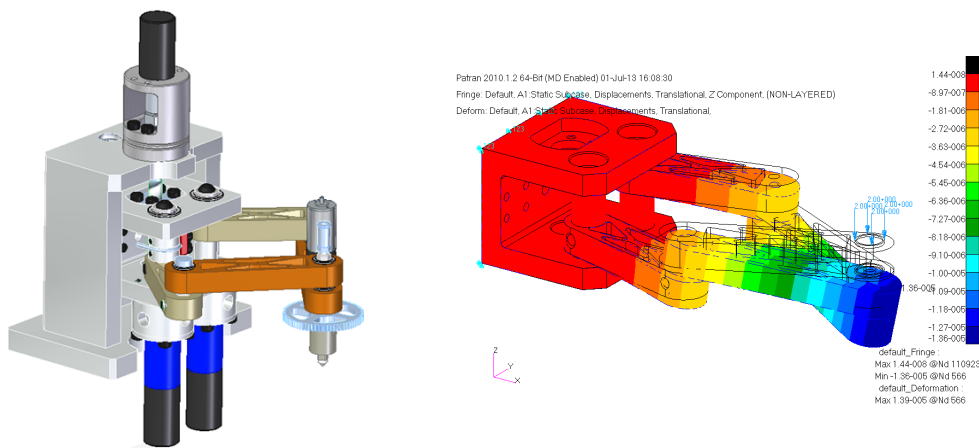


Figure 7: Virtual prototype of the precision manipulator and FEM analysis of the system

The changes made on the miniaturized-manipulator's structure concern the position of the motors actuating joint 1 and 2 (see Figure 7), the shape of the links, and the design of the passive and active joints. As an example, Figure 7 shows the results of the FEM analysis of preliminary new precision manipulator for a  $0.2\text{ kg}$  payload and with the end-effector located at the maximum allowed distance from the fixed frame; in particular the deflection along  $z$  axis is highlighted. The maximum displacement calculated is  $13.9\ \mu\text{m}$ ; it is a definitely acceptable value that could be improved optimizing the mechanical structure of the system.

## 6 CONCLUSIONS

During the research activity developed within the PRIN2009 project, the research group of the University of Bergamo has carried out the design of a 4DOFs miniaturized-manipulator for assembly and manipulation of extremely small components. The specific characteristics of this device are the very small dimensions, the small working volume, and the very accurate repeatability and resolution. The design process followed a typical mechatronic approach; according to such an approach, a synergistic interaction between the different part constituting the system is needed. In particular, the design focused on the integration of the drive systems within the mechanical frame, with particular

reference to the choice of the proper motor/transmission units to get the required performances. For the choice of the links' dimensions, an accurate kinematic and dynamic synthesis has been carried out, evaluating different methods and different local and global dexterity indices. Finally, the motor/transmission units has been chosen, and a preliminary prototype has been realized. In a short time, the experimental phase will begin at the aim to investigate the actual behavior of the manipulator and to validate its performances. At the same time, by means of a finite element analysis, we are designing new manipulator arms made of aluminum alloy in order to get an optimal balance between the lightness of the parallel structure and structural stiffness.

#### Acknowledgments

This research is funded by the Italian Ministry for Education, Universities and Research (MIUR) within the PRIN2009 Project "Micro Manipulation and Assembly MM&A".

#### References

- [1] Cecil, J. Powell, D. Vasquez, D. "Assembly and manipulation of micro devices A state of the art survey", *Robotics and Computer-Integrated Manufacturing*, **23**, 580-588, (2007)
- [2] Burisch, A., Raatz, A., Hesselbach, J., "Challenges of Precision Assembly with a Miniaturized Robot", *Proc. of 5th IFIP WG 5.5, IPAS 2010* Chamonix, France, pp 227-234, (2010).
- [3] Hesselbach, J., Raatz, A., Wrege, J., Soetebier, S. "Design and analysis of a macro parallel robot with flexure hinges for micro assembly tasks". *Proceedings of 35<sup>th</sup> International Symposium on Robotics (ISR)*, (2004).
- [4] Burisch, A., Wrege, J., Raatz, A., Hesselbach, J., Degen, R.: "PARVUS miniaturised robot for improved flexibility in micro production". *Journal of Assembly Automation*, **27(1)**, 6573 (2007)
- [5] Campos, L., Bourbonnais, F., Bonev, I.A., Bigras P., "Development of a Five-Bar Parallel Robot With Large Workspace", *Proc. Int. Design Engineering Technical Conferences and Computers and Information in Engineering Conference (IDETC/CIE2010)* Montreal, Canada, pp. 917-922 (2010)
- [6] Callegari M., Palpacelli M. and Scarponi M., "Kinematics of the 3-CPU parallel manipulator assembled for motions of pure translation", *Proc. Intl. Conf. Robotics and Automation*, Barcelona (2005)
- [7] Merlet, J.P., "Parallel Robots" 2<sup>nd</sup> edition, Springer ISBN: 978-1-4020-4132-7, (2006)
- [8] G., Legnani et al., "Micro manipulation and assembly", *Atti del 2° Congresso Nazionale del coordinamento della meccanica italiana*, 25-26 giugno 2012, ANCONA, (2012)
- [9] Siciliano, B., Khatib, O., "Springer Handbook of Robotics", ISBN 978-3-540-23957-4 (2008).
- [10] Van de Straete, H.J., Degezelle, P., De Schutter, J. "Servo motor selection criterion for mechatronic applications", *IEEE/ASME Trans. Mechatronics*, **3**, pp. 43-50 (1998)